Application of Multitemporal ERS-2 Synthetic Aperture Radar in Delineating Rice Cropping Systems in the Mekong River Delta, Vietnam

Soo Chin Liew, *Member, IEEE*, Suan-Pheng Kam, To-Phuc Tuong, Ping Chen, Vo Quang Minh, and Hock Lim, *Member, IEEE*

***Abstract*— In this paper, we report the use of multitemporal ERS-2 satellite synthetic aperture radar (SAR) images in delineating and mapping areas under different rice cropping systems in the Mekong River Delta, Vietnam. Change index maps were generated from seven images acquired between May and December 1996. Using a 3-dB threshold, the pixels in each change index (CI) map were classified into one of three classes: increasing, decreasing, or constant backscattering. Five of the CI maps were used to generate a composite map with 243 possible change classes. These change classes were grouped into thematic categories of rice cropping systems using two methods: human visual inspection and a semiautomatic hierarchical clustering algorithm. The derived thematic maps were compared with SPOT scenes acquired during the same rice seasons.**

***Index Terms*— Agriculture, clustering methods, image classification, remote sensing, synthetic aperture radar (SAR), vegetation mapping.**

I. Introduction

VIETNAM is one of the world's largest rice producing countries, and the fertile Mekong River Delta at the southern tip of Vietnam accounts for nearly half of the country's rice production. Rice cultivation in the Mekong River Delta is largely governed by hydrology, rainfall pattern, and the availability of irrigation [1]. As new water management infrastructure is being developed, the rice cropping systems in the Mekong River Delta have been undergoing rapid changes in recent years, with the tendency for greater intensification (i.e., growing more rice crops per year) and diversification (i.e., increasing the variety of crops planted). The consequence is a large variety of rice cropping systems reflecting the farmers' strategies in adjusting or optimizing their cropping practices under prevailing environmental and socioeconomic conditions.

Given the rapid changes that have been occurring, it is important for farming systems researchers as well as agriculture planners and land management officers to monitor spatially the change in cropping systems from year to year. The current practice in the compilation of rice cropping system maps in the regional and provincial levels involves massive deployment of workers to the fields to gather information about the farming practices. The use of satellite remote-sensing imagery acquired at the appropriate time would greatly help in the compilation and timely updating of such maps. Given the diversity of the cropping systems, it would be very difficult, if not impossible, to discriminate the areas under different planting systems using one single-date image. Multitemporal images are required to monitor the spatial and temporal growth patterns of the rice crops and, subsequently, to identify the cropping systems practiced at a particular region. Multispectral visible/near-infrared images such as those from the SPOT or LANDSAT satellites could be used for this purpose. Unfortunately, a large part of the rice growing season coincides with the rainy period, resulting in limited availability of cloud-free images throughout the growing season. The use of cloud penetrating synthetic aperture radar (SAR) would overcome this problem.

Various studies on the backscattering of radar from rice plants indicate that correlation exists between radar backscatter and plant biomass. Investigations using X-band airborne SAR in France [2] showed an increase of radar backscatter with time after transplantation that coincided with increase of biomass. The study by Kuroso *et al.* [3] in Japan showed a clear relationship between the radar backscattering coefficients and rice crop parameters using the C-band VV-polarized SAR onboard the ERS-1 satellite. Le Toan *et al.* [4] investigated the temporal behavior of ERS-1 SAR backscatter from rice crops in relation to the rice growing conditions for a tropical test site in Indonesia and a temperate site in Japan. They observed similar relations between radar backscatter and plant biomass for rice plants in these two different areas. The dependence of radar backscatter on rice plant growth stages have also been observed in studies conducted in South China using the C-band HH-polarized RADARSAT SAR [5] and in Malaysia using ERS-1 SAR [6]. Theoretical simulation [4] shows that the scattering mechanism for C-band VV-polarized SAR is dominated by double scattering between the water surface and the rice plants. The backscattering coefficient increases from -16 dB or less at the beginning of the growth cycle when the field is inundated and there is little biomass in the field to about -8 dB at the saturation level [4]. Hence, it should be possible to monitor the rice growth stage by measuring the backscattering coefficient from the plants as

Manuscript received November 24, 1997; revised May 12, 1998.

S. C. Liew, P. Chen, and H. Lim are with the Centre for Remote Imaging, Sensing, and Processing, National University of Singapore, 119260 Singapore (e-mail: phyliew@leonis.nus.edu.sg).

S.-P. Kam and T.-P. Tuong are with the International Rice Research Institute, 1099 Manila, Philippines.

V. Q. Minh is with the Department of Soil Science, Faculty of Agriculture, University of Can Tho, Can Tho, Vietnam.

Publisher Item Identifier S 0196-2892(98)06836-3.

TABLE I
MAIN RICE SEASONS IN THE MEKONG RIVER DELTA

Rice Crop	Local Name	Variety	Planting Method	Planting	Harvest
Winter - Spring	*Dong Xuan (DX)*	Modern	Direct seeding	Nov/Dec	Feb/Mar
Summer - Autumn	*He Thu (HT)*	Modern	Direct seeding	May/Jun	Aug/Sep
Rainy Season	*Mua (M)*	Traditional	Transplanting	Jul/Aug	Dec/Jan
	Thu Dong (TD)	Modern	Direct seeding or transplanting	Sep/Oct	Nov/Dec

TABLE II
MAIN RICE-BASED CROPPING SYSTEMS IN THE STUDY AREA

Rice-Based Cropping System	Rice Seasons
SINGLE RICE CROP	
Rainfed	*Mua (M)*
DOUBLE RICE CROP	
Rainfed	*He Thu (HT) Thu Dong (TD)* wDSR *He Thu (HT) – Thu Dong (TD)* dDSR *He Thu (HT) – Thu Dong (TD)*
Irrigated	*Dong Xuan (DX) - He Thu (HT)*
TRIPLE RICE CROP	
Irrigated	*Dong Xuan (DX) - He Thu (HT) – Thu Dong (TD)*
RICE-SHRIMP SYSTEM	
Rice-shrimp pond	*Mua (M)*
Rice-shrimp pond- upland crop	*Mua (M)*

a function of time if radar images are acquired at appropriate time intervals. Generally, the beginning of a rice season would be identified by a low backscatter in the time series when the field was inundated, while the end of the reproductive stage is characterized by a high backscatter.

The objective of this paper is to delineate and map the spatial distribution of the various rice cropping systems in the Mekong River Delta using a series of ERS-2 SAR imagery acquired in 1996. The delineation and classification of the rice cropping systems was based on the thresholding of change index (CI) maps derived from the multitemporal SAR images. For a given rice area, the temporal change pattern of its radar backscatter provides a signature that enables its cropping system to be identified. In Section II, a brief description of the rice cropping systems practiced in the Mekong River Delta is provided. The image processing and rice cropping system classification methods are described in Sections III and IV, respectively. The results of rice cropping systems classification and the interpretation of the classification results are discussed in Section V. This section also includes comparisons with available optical images acquired by the SPOT satellites.

II. RICE CROPPING SYSTEMS IN THE MEKONG RIVER DELTA

The Mekong River Delta receives 1600–2000 mm of rain annually, with the rainy season starting in May and lasting until November. The main rice seasons in the Mekong River Delta are listed in Table I. The TD crop is a variation of the traditional Mua (M) crop, whereby short-duration modern varieties are used instead of the local, long-duration varieties. These three rice seasons, in various combinations governed by hydrology, rainfall pattern, and availability of irrigation, constitute the variety of rice-based cropping systems practiced in the Mekong River Delta [1]. The rice cropping systems vary from the single rainfed rice crop in the coastal fringes to the double rainfed rice, double and triple irrigated rice crops, and even more intense and more diverse cropping systems involving rice with shrimp culture and with upland crops.

Table II summarizes the major rice cropping systems practiced in the study area. The single rice crop is invariably the M, which is practiced in the tidally inundated coastal areas that are subjected to saline water intrusion prior to the rainy season. The double cropping system may be the Dong Xuan-He Thu (DX-HT) or the HT-Thu Dong (HT-TD) system. As the DX crop grows during the dry season, the DX-HT cropping system is practiced in areas that receive irrigation water. The HT-TD system is practiced under predominantly rainfed conditions. The crop calendar varies each year, depending on the onset of the rainy season for the start of the HT crop. The HT crop is direct-seeded. In the dry direct seeding (dDSR) method, the seeds are sown onto dry fields prior to the start of the rainy season. Alternatively, the pregerminated seeds are sown onto wet fields in the wet direct seeding (wDSR) method. Due to differences in sowing dates (dDSR is carried out earlier than wDSR), in the initial field wetness condition, as well as in the initial crop growth rates (wDSR crop establishes faster), these two direct seeding methods would exhibit different radar backscattering characteristics at the early part of the crop season. The TD crop may be transplanted or wet direct seeded. The triple crop system combines all three rice seasons (DX-HT-TD) and is practiced in areas with favorable hydrological conditions and available irrigation facilities.

III. DATA COLLECTION AND SAR IMAGE PROCESSING

Seven descending mode ERS-2 SAR images at 35-day repeat intervals were acquired (track 75, frame 3411 shifted along track by 30% to cover areas of interest, see Fig. 1 and inset for the location map) during the following dates in 1996: May 5, June 9, July 14, August 18, September 22, October 27, and December 1. Reasonably cloud-free SPOT multispectral images of parts of the study area were also acquired on June 19, 1996, November 5, 1996, and January 28, 1997. These optical images were used to aid in the interpretation of the SAR images.

Ground truthing field trips were carried out on dates coincidental with or close to the dates of SAR image acquisition. Over 90 plots of rice fields, each about 100×100 m^2 in size were monitored for general field conditions, date of planting, and crop growth stages. As it was not possible to make field observations to cover comprehensively the entire 100- $\times$ 100-km ERS scene, an ex-post field check was carried out after completion of the SAR image processing and classification to confirm the delineated spatial pattern of the rice cropping systems, with consultation with the local agricultural extension offices.

The ERS-2 scenes were acquired and processed into the calibrated SAR precision image (PRI) format at the ground station of the Centre for Remote Imaging, Sensing, and Processing (CRISP), Singapore. Each PRI product was first converted

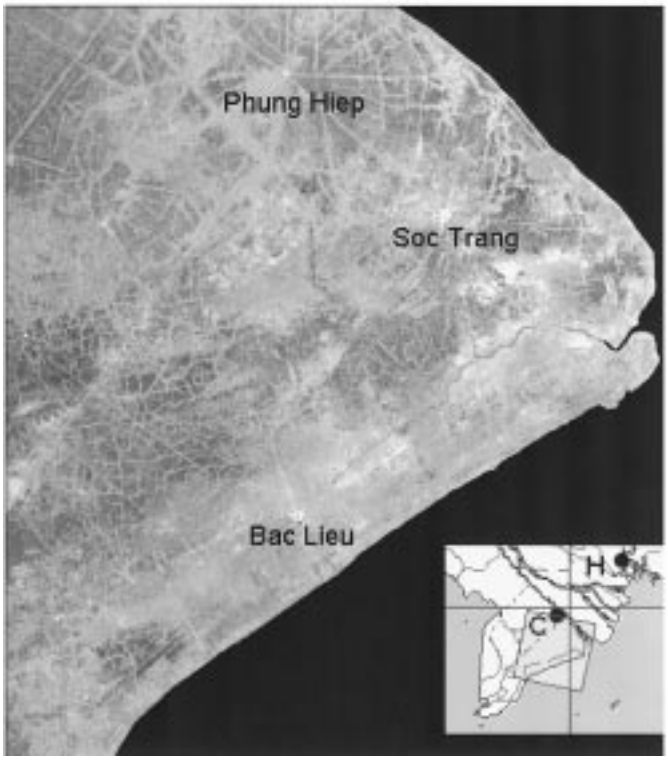

Fig. 1. Multitemporal ERS-2 SAR color composite image of the test area. (Red: May 5, Green: June 9, Blue: July 14, 1996). Inset: Location map of the test area. C: Can Tho City, H: Ho Chi Minh City. All ERS scenes: © 1996, ESA.

to 8-bit images by dividing the 16-bit pixel digital numbers (DN's) by four, lowpass filtered using a 5×5 averaging window and then downsampled to 50-m pixel size. An edge-preserving speckle removal filter based on the adaptive Wiener filter for multiplicative noise was applied followed by a 3×3 median filter. For ease of analysis, parts of the sea and the Cu Lao Island on the bank of the Hau Giang (the southernmost branch of the Mekong River) appearing in the scene were masked out. The variety of rice cropping systems practiced in the study area is illustrated by the multitude of colors in the multitemporal color composite image shown in Fig. 1, which is composed of the ERS images of May 5, June 9, and July 14 displayed in the red, blue, and green bands, respectively.

IV. Classification of Rice Cropping Systems

A. Generation of Change Classes

Classification of the rice cropping systems in this region was based on thresholding the CI's derived from the series of multitemporal SAR images. For each consecutive pair of images 1 and 2, a CI map was generated. The CI was defined as the change in the backscattering coefficient expressed in decibels

$$\mathrm{CI} = \Delta\sigma^o\ (\mathrm{dB}) = 20\ \log_{10}(\mathrm{DN2/DN1}) \tag{1}$$

where DN1 and DN2 are the pixel DN's of the images 1 and 2, respectively. Six CI maps were generated from the series of seven SAR images. An arbitrary threshold was then applied to each CI map to produce a threshold-change-index (TCI) map. A threshold value of 3 dB was found suitable for delineating the different classes of rice cropping systems. For each TCI map, the pixels were classified as having a constant (-3 dB $<$ CI $<$ $+3$ dB), decreasing (CI ≤ -3 dB) or increasing (CI $\geq +3$ dB) backscattering over the corresponding time period. Five TCI maps (covering the period from June 9 to December 1) were used in the classification. By combining these five TCI maps, 243 (i.e., 3^5) possible classes could be formed. Each pixel was assigned a class number according to

$$\text{Class No.} = \sum_i 3^{i-1} t_i \tag{2}$$

where t_i ($i = 1, 2, \cdots, 5$) is the pixel value of the ith TCI map, which assumes one of the values zero (constant backscatter), one (decreasing backscatter), or two (increasing backscatter). Since these classes were obtained from the TCI's, they will be referred to as the "change classes."

B. Grouping of Change Classes into Thematic Classes

The next step in the classification procedure is to group the change classes with similar temporal backscatter change pattern into a thematic category of land cover type, with emphasis on the rice cropping systems. Two approaches were employed.

The first approach attempted was by visual inspection of the time series of radar backscattering coefficient (σ_0 in decibels) for each change class associated with rice cropping and interpreting it in relation with known crop calendars and local knowledge of the general geographical pattern of the various rice-based cropping systems [7]. This manual method is practicable for the dominant change classes, i.e., those with high pixel membership and distinct spatial clumping patterns. It became difficult to discern the associated cropping system for change classes that have a low number of pixels, particularly if these are widely scattered within the scene. This method would result in a thematic map that could be considered preliminary because of a substantial proportion of unclassified pixels belonging to the minority change classes.

A clustering algorithm was therefore devised to group the change classes based on the similarity of their CI time series. This is based on the assumption that change classes with similar change patterns in their backscatter time series are likely to represent similar cropping systems; the subtle differences reflecting the spatial and temporal heterogeneity arising from field-to-field variation. The input to this algorithm is the time series of the N change classes. Each class is characterized by the mean values $x_{i,n}$ and standard deviation $s_{i,n}$ of its CI at time interval i. The population of class n is c_n. The aim of the algorithm is to cluster these N classes into M nonoverlapping groups ($M \leq N$), i.e., any class n can be a member of exactly one group. A distance measure for the "closeness" of two time series m and n is defined as

$$D_{mn} = \sqrt{\sum_i \frac{(x_{i,m} - x_{i,n})^2}{s_{i,m}^2 + s_{i,n}^2}}. \tag{3}$$

Given a threshold distance D_0, two classes m and n should be grouped together if $D_{mn} \leq D_0$. After grouping the two classes, the population, mean and standard deviation of the new group are, respectively

$$C = c_m + c_n \tag{4}$$

$$X_i = \frac{c_m x_{i,m} + c_n x_{i,n}}{C} \tag{5}$$

and

$$S_i = \sqrt{\frac{1}{C}\left(c_m s_{i,m^2} + c_n s_{i,n^2} + \frac{c_m c_n (x_{i,m} - x_{i,n})^2}{C}\right)}. \tag{6}$$

At the initialization of the clustering algorithm, the class $n = 1$ is taken as the starting group and $M = 1$. Starting from $n = 2$, the following steps are iterated until $n = N$.

1) Find the group k among the existing M groups that is closest to the class n, i.e., D_{kn} is a minimum.
2) Test whether the distance between class n and group k is greater than the threshold distance. If $D_{kn} \leq D_0$, proceed to Step 3), otherwise go to Step 4).
3) If $D_{kn} \leq D_0$, class n is merged into group k. The new mean, sd, and population of the group k are computed according to (4) to (6). Increment n by one and go to Step 1).
4) If $D_{kn} > D_0$, the class n forms a new group, M is incremented by one, and the new group is labeled by the new M. Increment n by one and go to Step 1).

The results of this clustering technique would depend on the value of the threshold distance D_0. A larger threshold value would result in fewer clusters with higher number of change classes, whereby it is likely that change classes belonging to different cropping systems would be clustered together. On the other hand, if the threshold were set too small, the more stringent condition would result in too many clusters. We found that a good strategy is to employ a hierarchical approach in merging the change classes. A more lenient threshold is first chosen to group the change classes into several clusters. The clusters are visually examined, both for the backscatter time series of the member change classes as well as their grouping and geographical association with the preliminary thematic map obtained by the manual method described above. Where necessary, i.e., where change classes belonging to a cluster are found to have still distinct differences in backscatter time series and geographical distribution, a second or even a third clustering would then be performed using smaller threshold value(s) to obtain subclusters. Hence, the hierarchical approach requires user intervention and the decision whether to subcluster depends on visual interpretation.

V. Results and Discussion

A. Delineation of Rice Cropping Systems

Altogether, 204 out of the 243 possible change classes occurred within the study area. The change class of value zero corresponds to pixels in which the radar backscattering coefficient remained relatively constant throughout the period of observation. These are associated with the nonrice areas with relatively invariant surface features, such as the built-up areas, Melaleuca forests, and perennial trees.

TABLE III
Grouping of Change Classes into Thematic Categories of Land Cover and Rice Cropping Systems by Visual Inspection

Thematic Class of Rice Cropping System	Change Classes	No. of CC (Percent of Change Pixels)
Single Crop Rainfed Rice *Mua*	**1, 7, 163, 169**	4 (14.97%)
Double Crop Rainfed Rice wDSR early *HT-TD*	**191, 29, 209, 2, 164**	5 (11.36%)
Double Crop Rainfed Rice wDSR late *HT-TD*	**190, 196**	2 (2.78%)
Double Crop Rainfed Rice dDSR *HT-TD*	**33, 195, 45, 207,** *208*	5 (10.60%)
Mixed Double Crop Rice (Irrigated & Rainfed)	**27, 189**	2 (22.57%)
Mixed Double Crop & Ttriple Crop Rice (Irrigated)	**192, 210, 212, 194**	4 (4.86%)
Rice-Shrimp	**18, 19, 21**	3 (3.33%)
Rice-Shrimp-Upland Crop	**54,** *61*	2 (1.84%)
Upland Crop	**162**	1 (4.69%)
Orchard	**81**	1 (6.22%)
	Total	**29 (83.25%)**

Change classes printed in bold have been classified into the same thematic categories for both the visual inspection method and the hierarchical clustering approach (Table IV). Change classes printed in italics are those for which a discrepancy occurs between the two approaches.

Thirty of the 204 change classes account for 86.7% of the nonzero pixels, i.e., where the CI for at least one of the series of five TCI maps exceeds the threshold value of 3 dB. Twenty-nine of these 30 dominant change classes were grouped by visual inspection into ten land use and rice cropping system categories, as summarized in Table III. Change class 6 (containing 3.46% of the nonzero pixels) remained unclassified because of its indistinct backscatter time series pattern and the very scattered distribution pattern of its pixels. In the resulting thematic map, almost 17% of the nonzero pixels would have remained unclassified.

The hierarchical clustering technique was employed to improve the thematic mapping. A threshold distance of 2.5 was initially used to cluster those change classes with 100 pixels or more. This procedure resulted in 33 clusters, of which cluster 1 consists of the single change class with value zero. Of the remaining 32 clusters, the top 18 (in terms of pixel numbers) accounted for 94 change classes comprising almost 99% of the nonzero pixels. Only these clusters were subjected to further analysis. There were four cases in which, upon visual examination, hierarchical subclustering was further applied by using lower threshold distances. Land use and rice cropping system categories are assigned to the resulting clusters, as summarized in Table IV, by considering the correspondence of the change pattern of the backscatter time series with the

TABLE IV
GROUPING OF CHANGE CLASSES INTO THEMATIC CATEGORIES OF LAND COVER AND RICE CROPPING SYSTEMS USING A HIERARCHICAL CLUSTERING ALGORITHM

Thematic Class of Rice Cropping System	Cluster No.	Change Classes in Cluster	No. of CC (Percent of Change Pixels)
Single Crop Rainfed Rice Mua	#2 #28 #17b #17c #17d #6b #22	**1**, **7**, 16, **169** **163**, 181 55, *61*, 64, 70 136, 142, 151, 150 172, 10 82, 88	18 (17.42%)
Double Crop Rainfed Rice wDSR early HT-TD	#3 #7 #9	**2**, 8, **164**, 170, **191**, **29**, 35, 197 11, 17, 173, 179, 200, 206 20, 47, 53, **209**, 215	19 (13.81%)
Double Crop Rainfed Rice wDSR late HT-TD	#13	28, 34, **190**, **196**, *208*, 214, 46, 52	8 (4.81%)
Double Crop Rainfed Rice dDSR HT-TD	#12a2 #12a3 #12b #6a #32	**33** **195** **45**, 51, **207**, 213 9, 15, 171, 177 198, 204	12 (12.08%)
Mixed Double Crop Rice (Irrigated & Rainfed)	#12a1	**27**, **189**	2 (22.57%)
Mixed Double Crop & Triple Crop Rice (Irrigated)	#31 #4b #4c	**192**, **194**, **210**, **212** 30, 48 165, 167, 183, 185	10 (5.83%)
Rice-Shrimp	#8 #4a	**18**, **19**, 22, 180 3, 5, **21**, 23	8 (4.44%)
Rice-Shrimp-Upland Crop	#17a #18	**54**, 60, 63, 69, 135, 141, 144 56, 62, 65, 71, 137	12 (1.96%)
Upland Crop	#27	**162**	1 (4.69%)
Orchard	#21	**81**	1 (6.22%)
		Total	**91 (93.85%)**

Change classes printed in bold have been classified into the same thematic categories using both the visual inspection method (Table III) and the hierarchical clustering approach. Change classes printed in italics are those for which a discrepancy occurs between the two approaches. Change classes printed in regular font are the additional classes not included in the visual inspection method.

crop calendars as well as the geographical distribution pattern of their associated pixels. Cluster 5, which is dominated by change class 6, remained unclassified because of the very scattered distribution pattern of its pixels.

Comparison of Tables III and IV shows that there is a close correspondence between the assignment of change classes to land use/rice cropping system categories using the manual method and that assisted by the hierarchical clustering technique, with the exception of two cases, i.e., change classes 61 and 208. In fact, the clustering technique helped in clarifying the ambiguous assignment of these two change classes in the thematic categories using visual inspection because of the scattered nature of their associated pixels. It is also obvious from Table IV that the hierarchical clustering technique enabled many more minority change classes to be included into the various thematic categories based on the resemblance of their backscatter time series. This constitutes an effective statistical averaging technique for handling local, field-to-field variation. The resulting thematic map of the rice cropping systems is shown in Fig. 2.

Most of the major rice cropping systems listed in Table II have been delineated. Even variations of the double-cropped rainfed HT-TD cropping system have also been identified. On the other hand, the irrigated triple crop and double crop systems could not be separated, and the irrigated DX-HT was confused with the rainfed HT-TD system in some areas. Also, the change class of value zero represents all surface features with relatively time-invariant backscatter characteristics and does not distinguish between land cover features, such as built-up areas, forests, rivers, and roads. The typical backscatter time series of the change classes for each thematic category of rice cropping system are shown in Fig. 3(a)–(g).

B. Interpretation of Radar Backscatter Time Series

The backscatter time series for the single rice cropping system (rainfed M, colored red in Fig. 2), is characterized by a sharp drop in the radar backscatter coefficient (σ^o) between June 9 and July 14 [see Fig. 3(a)], corresponding with the start of the M rice crop when the fields were cleared of weeds, ploughed, harrowed, and then flooded before transplanting was carried out. The backscatter then increased and remained high for the rest of the monitoring period when the crop was in the field.

Three variations of the double crop rainfed HT-M systems were distinguishable because of their distinctive backscatter time series. Two of the variations are associated with areas where wDSR of the HT crop was practiced [Fig. 3(b) and (c)]. Both sets of backscatter time series show two distinct drops in σ^o. The first drop [in the June 9 scene in Fig. 3(b) and in the July 14 scene in Fig. 3(c)] marks the start of the wDSR HT crop, which is sown in flooded field conditions; hence, the low σ^o. The σ^o values increased with the growth of the HT crop and then dropped in the October 27 scene after its harvest. The subsequent increase in σ^o after October corresponds with the growth of the TD crop. The backscatter time series shown in Fig. 3(b) corresponds with the bright green areas in Fig. 2, where the HT crop was planted earlier, in lower-lying areas where flooding started earlier, in late May/early June. The dark green areas are where the HT crop was planted later.

The third variation of the rainfed HT-TD cropping system is indicated by the cyan-colored areas in Fig. 2. This is associated with areas of relatively higher ground where the HT crop was dry direct seeded and there was no early season inundation of the rice fields. The drop in σ^o [Fig. 3(d)] was not as sharp as for the wDSR HT areas [Fig. 3(b) and (c)]. The dry-seeded HT crop usually takes a longer time to accumulate biomass and canopy volume; hence, the slower rate of increase in σ^o over the June–August period. The drop in backscatter in October corresponds with the transition to the TD crop.

The backscatter time series in Fig. 3(e) corresponds with the yellow areas in Fig. 2, where two types of rice cropping systems occur under irrigated conditions, i.e., the triple DX-HT-TD system and the double DX-HT system. The irrigated DX-HT system is practiced in the lower lying areas that are subjected to severe flooding in September/October. The HT crop is planted early, in April, and is harvested in August before deep flooding occurs. Correspondingly, σ^o increased

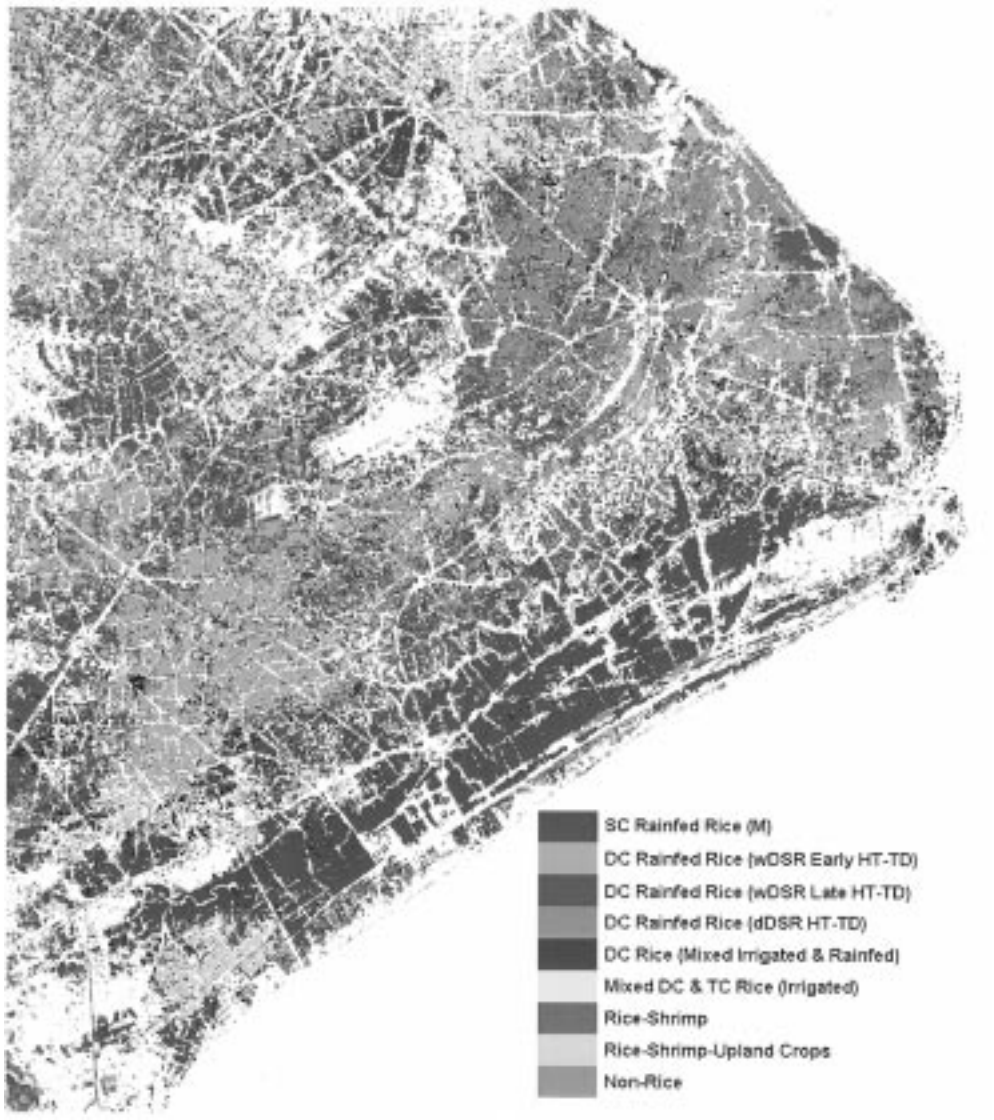

Fig. 2. Thematic classes of rice cropping systems in the Mekong River Delta obtained by hierarchical clustering of the change classes derived from five SAR threshold-change-index maps. See Table IV and text for the rice cropping systems corresponding to each color in the map, and see Fig. 3 for the typical backscattering time series.

from May 5, peaked at July 14, and dropped in the August 18 scene. The fields remain fallow until the planting of the DX crop after subsidence of the flood in November/December. The increase in σ^o between August 18 and September 22 is probably due to weed emergence. The drop in σ^o at the end of October coincides with the peak of flooding, while the subsequent increase in σ^o in December marks the start of the DX crop. The same backscatter time series is also associated with the triple DX-HT-TD crop. In this case, the increase followed by the drop in σ^o between May and August corresponds with the HT crop, while the second increase followed by the drop in σ^o between August and late October corresponds with the TD crop. The subsequent increase in σ^o marks the start of the DX crop.

The backscatter time series in Fig. 3(f), corresponding to the magenta-colored areas in Fig. 2, is also associated with two different rice cropping systems, i.e., the rainfed HT-TD and the irrigated DX-HT. However, this backscatter time series lacks the dip in σ^o at the start of the rainy season, as shown in Fig. 3(b) and (c), which would be expected at the start of the rainfed HT crop. A plausible explanation is that the dip had not been captured, given the 35-day interval between two consecutive ERS acquisition dates. This backscatter time series is also associated with a variation of the irrigated DX-HT cropping system, which is practiced in areas that are not severely affected by flooding during the rainy season, where the HT crop is planted later (in May/June) to take advantage of the rains. The increasing σ^o from July to September corresponds with the growth of the HT crop. The drop in σ^o on October 27 corresponds with the onset of flooding after the harvest of the HT crop.

The shrimp-rice system (colored brown in Fig. 2) is practiced in the low depression areas. Shrimp is cultivated in ponds during the dry season. The M rice crop is transplanted late, usually in July after the harvest of the shrimps and the flushing out of saline water by the rains. The backscatter

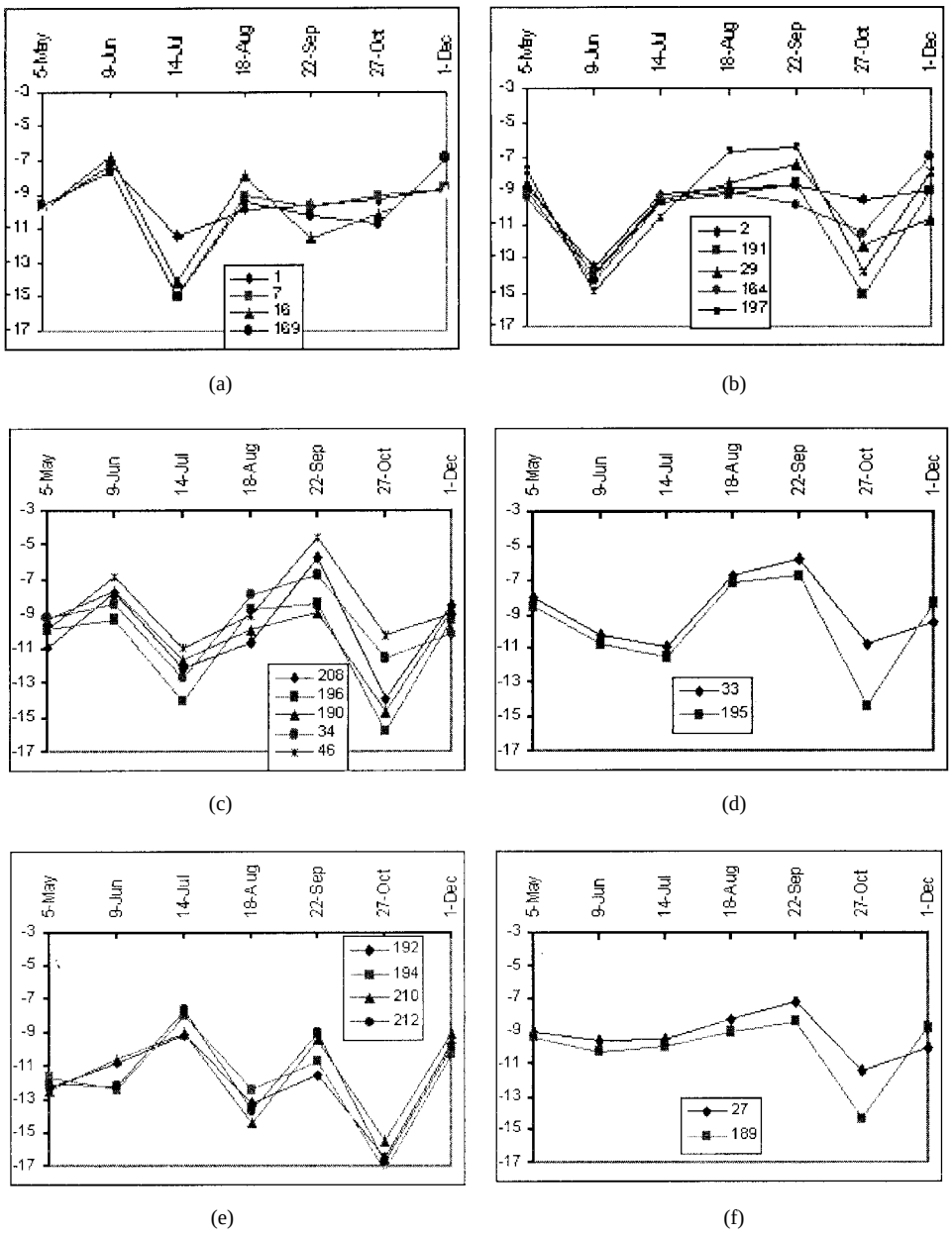

Fig. 3. Representative backscattering time series of the change classes constituting the major thematic classes of rice-based cropping systems. The vertical axis in each graph is the class average backscattering coefficient in decibels for the change classes. The standard deviations of most data points range from 1 to 2 dB. (a) Single crop: rainfed M; (b) double crop: rainfed wDSR early HT-TD; (c) double crop: rainfed wDSR late HT-TD; (d) double crop: rainfed dDSR HT-TD; (e) mixed double and triple crops; and (f) double crop: mixed irrigated and rainfed.

pattern is variable between June and August, depending on the surface condition of the shrimp ponds. The backscatter increases from August until early December, corresponding with the growth of the M crop. The shrimp-rice-upland crop system is a variation whereby upland crops, annuals, and perennials are grown on the bunds. The presence of these upland crops modifies the radar backscatter in different ways, depending on the crop type and crop geometry.

C. Comparison with Optical Imagery

The interpretation of the radar backscatter time series was based on field observations and knowledge of the cropping systems, crop calendars, and farming practices. As it was not possible to have field observations covering all areas within the 100- $\times$ 100-km ERS scene, the three multispectral SPOT scenes acquired for the study area provided a global view of the ground conditions. Fig. 4(a)–(c) show the coregistered SPOT scenes for a common overlapping subarea of 58 $\times$ 50 km, in comparison with the corresponding subset of the thematic map derived from the multitemporal ERS data [Fig. 4(d)].

The January SPOT scene, in particular, distinguishes very clearly the rainfed rice area closer to the coast from the irrigated and partially irrigated rice area further inland. By January, all rainfed rice crops have been harvested. The reddish tones correspond with areas of the irrigated DX and the remaining late-planted TD crop that received supplemental

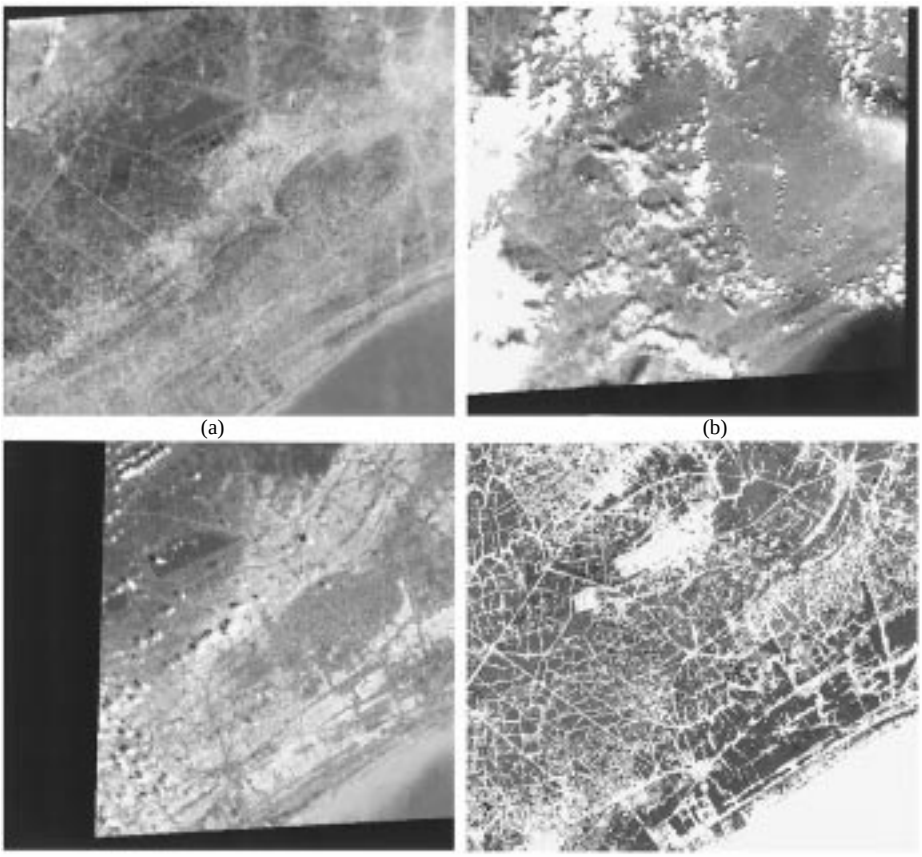

Fig. 4. (a) June 19, 1996, SPOT scene; (b) November 7, 1996, SPOT scene; (c) January 28, 1997, SPOT scene; and (d) subset of the thematic map of rice cropping systems derived in this study; see Fig. 2 for legends. The SPOT images and the thematic map have been coregistered together. All SPOT scenes: © 1996, 1997 CNES, acquired and processed by CRISP Singapore, distributed by SPOTIMAGE/SPOTAsia.

irrigation water. This image indicates an opportunity for separating the mixed thematic classes obtained from the May-December multitemporal ERS SAR data, with the incorporation of at least one dry season image. A slightly later acquisition date, in February, would be more suitable to isolate the irrigated DX crop. The June 19 SPOT scene confirms the separation between the single rainfed rice area (nonvegetated strip near to the coast) from the double rainfed area (vegetated/partially vegetated regions further inland in tones of red), and between the early-HT (partially vegetated with darker tone) and late-planted HT (fully vegetated with brighter tone) areas. The November SPOT scene distinguishes the reddish tone of the TD and M crops of the rainfed rice cropping systems from the irrigated areas, which were in fallow.

VI. Summary and Concluding Remarks

In conclusion, the dominant rice cultivating systems practiced in the study area have been delineated by thresholding the CI maps derived from multitemporal SAR images. The thresholding process produced change classes characterized by their unique signature of radar backscatter time series. The change classes were merged into one of the several thematic classes of rice cropping systems based on their similarity in the backscatter time series and their geographical distribution. Two methods of grouping the change classes have been investigated. The first method used human interpretation of the radar backscatter time series, together with knowledge of field conditions and crop calendars. The second method utilized a semiautomatic, hierarchical clustering algorithm, whereby user-selected threshold distance values were applied iteratively to cluster and subcluster the change classes where deemed necessary, from visual inspection of the resulting clusters. This hierarchical clustering method has been able to reproduce closely the results of clustering by human interpreters, with the added advantage of classifying numerous, more minority change classes that were difficult to categorize visually and would therefore otherwise remain unclassified.

Ambiguity still exists in assigning some change classes to their respective thematic classes due to insufficient temporal resolution of the repeat-pass ERS-2 scenes, in particular, between one of the rainfed HT-TD systems and the irrigated DX-HT system, and between the irrigated double rice and irrigated triple rice cropping systems. An acquisition during the dry season, at the peak of the DX crop, is needed to resolve this ambiguity, as is indicated by the January 28 SPOT imagery. Use of ascending mode images may help to increase the temporal resolution of the backscatter time series. However, mixing the two modes of acquisition may complicate the interpretation of the backscatter time series due to the different orientations of the ground with respect to the SAR line of sight and the possibility of nontrivial incidence

angle effects of the rice crops. Seasonal nonrice activities (e.g., sugar canes, shrimp ponds, and vegetable crops) may also confuse the interpretation of the radar backscatter time series. Furthermore, the emergence of weeds during period of land fallow may be confused with rice.

We had the luxury of acquiring every ERS-2 descending-pass scene of the test area from May to December during the rice growing seasons in 1996. The question remains as to what is the minimum number of scenes required for monitoring the rice cropping systems in an area as varied as the Mekong River Delta. Another operational satellite with SAR is the Canadian RADARSAT. The RADARSAT SAR has multiple incidence angle capability, and it is operated in the HH-polarization mode, in contrast to the single incidence angle and VV-polarization of the ERS satellite. The different polarization and incidence angle of RADARSAT may provide complimentary information useful in monitoring the growth stages of rice. We are currently investigating this possibility of combining RADARSAT and ERS SAR images for the purpose of rice monitoring and land cover classification.

REFERENCES

[1] T. P. Tuong, C. T. Hoanh, and N. T. Khiem, "Agro-hydrological factors as land qualities in land evaluation for rice cropping patterns in the Mekong Delta of Vietnam," in *Rice Production on Acid Soils of the Tropics*, P. Deturck and F. N. Ponnamperuma, Eds. Kandy, Sri Lanka: Inst. Fundamental Studies, 1991.

[2] T. Le Toan, H. Laur, E. Mougin, and A. Lopes, "Multitemporal and dual-polarization observations of agricultural vegetation covers by X-band SAR images," *IEEE Trans. Geosci. Remote Sensing*, vol. 27, pp. 709–717, May 1989.

[3] T. Kurosu, M. Fujita, and K. Chiba, "Monitoring of rice crop growth from space using ERS-1 C-band SAR," *IEEE Trans. Geosci. Remote Sensing*, vol. 33, pp. 1092–1096, Sept. 1995.

[4] T. Le Toan, F. Ribbes, L.-F. Wang, N. Floury, K.-H. Ding, J. A. Kong, M. Fujita, and T. Kurosu, "Rice crop mapping and monitoring using ERS-1 data based on experiment and modeling results," *IEEE Trans. Geosci. Remote Sensing*, vol. 35, pp. 41–56, Jan. 1997.

[5] Y. Shao, C. Wang, X. Fan, and H. Liu, "Estimation of rice growth status using RADARSAT data," in *Proc. 1997 IEEE Int. Geosci. Remote Sensing Symp.*, vol. 3, pp. 1430–1432.

[6] S. Bahari, A. Talib, H. T. Chuah, and H. T. Ewe, "A preliminary study of phenological growth stages of wetland rice using ERS1/2 SAR data," in *Proc. 1997 IEEE Int. Geosci. Remote Sensing Symp.*, vol. 2, pp. 1069–1071.

[7] S. C. Liew, S.-P. Kam, T.-P. Tuong, P. Chen, V. Q. Minh, L. Balababa, and H. Lim, "Delineation of rice cropping systems in the Mekong River Delta using multitemporal ERS SAR," in *Proc. 3rd ERS Symp.*, Florence, Italy, ESA SSP-414, Mar. 17–21, 1997, pp. 153–158.

Soo Chin Liew (M'93) received the Ph.D. degree in physics from the University of Arizona, Tucson, in 1989.

He was a Research Scientist at the Department of Radiology, University of California, San Francisco, before joining the Physics Department, National University of Singapore (NUS). He is currently a Research Fellow and Leader of the Vegetation and Forestry Research Group, Centre for Remote Imaging, Sensing, and Processing, NUS. He has worked on problems in tomographic image reconstruction, noise analysis, and computer simulation studies of image formation processes. His present research interests include SAR applications in agriculture and forestry, atmospheric effects, and image texture analysis.

Suan-Pheng Kam received the Ph.D. degree in agronomy from Cornell University, Ithaca, NY.

She was a Lecturer, then an Associate Professor at the University of Science, Malaysia, from 1981 to 1994. She underwent a certificate course on remote sensing at the Asian Institute of Technology, Bangkok, in 1984; was a visiting faculty at the Environmental Remote Sensing Center, University of Wisconsin, Madison, in 1986; and was at Imperial College under the Royal Society Fellowship in 1990. In 1994, she joined the International Rice Research Institute, where she is the GIS Specialist, Manila, Philippines, with the main responsibility of providing GIS and remote-sensing support to rice research.

To-Phuc Tuong received the Ph.D. degree in soil and water engineering from the University of Canterbury, New Zealand.

He was Associate Professor in the Department of Water Management, National Institute of Agriculture, Saigon, Vietnam, from 1973 to 1975. He was also Professor and Chairman of the Department of Water Management, University of Agriculture and Forestry, Ho Chi Minh City, Vietnam, from 1976 to 1991, when he joined the International Rice Research Institute, Manila, Philippines, as Water Management Engineer at the Soil and Water Sciences Division. His research interests include agrohydrology, water use for land reclamation, and land and water planning and management.

Ping Chen received the B.Eng. degree from Beijing Electronic Engineering College, Beijing, China, in 1983 and the M.Sc. degree in remote sensing from Beijing Agricultural University in 1987.

She joined the Centre for Remote Imaging, Sensing, and Processing, National University of Singapore, in 1995. She has been working on projects in vegetation and agricultural studies using remote sensing and forest fire monitoring. Her research interests include image processing and remote-sensing techniques.

Vo Quang Minh received the B.S. degree in agriculture (soil science) from Cantho University, Vietnam, and the M.S. degree in agriculture (soil science) from the University of the Philippines, Los Banos.

He has been a faculty member of the Department of Soil Science, Cantho University, since 1983, first as Instructor/Researcher and, subsequently, as Senior Lecturer and Vice-Chairman of the Department. His research interests are in soil classification and GIS-based land evaluation.

Hock Lim (M'94) received the B.Sc. degree in physics from the then University of Singapore and the Ph.D. degree in atmospheric science from the University of Reading, Reading, U.K.

He is currently Associate Professor in the Department of Physics and Director of the Centre for Remote Imaging, Sensing, and Processing, National University of Singapore. He has performed research on modeling and theoretical analysis of atmospheric phenomena, including the dynamics of the interactions between high-latitude and tropical atmospheric motions, numerical weather analysis and prediction, and nonlinear phenomena in fluid dynamical systems. His research interests also include image restoration and fundamental problems in remote sensing, such as the atmospheric effects on optical data and radar interactions with surfaces.